

Article

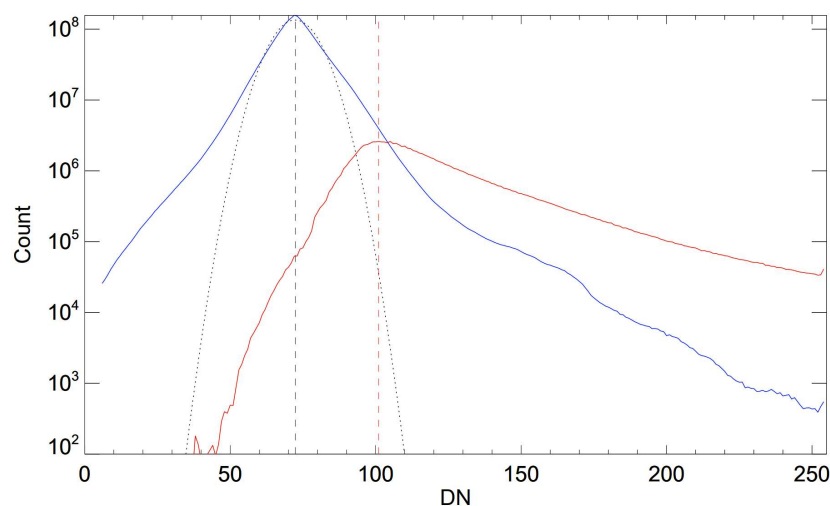
# Cloud Masks Derived from the Mars Daily Global Maps and an Application to the Tropical Cloud Belt on Mars

Huiqun Wang \* and Gonzalo González Abad

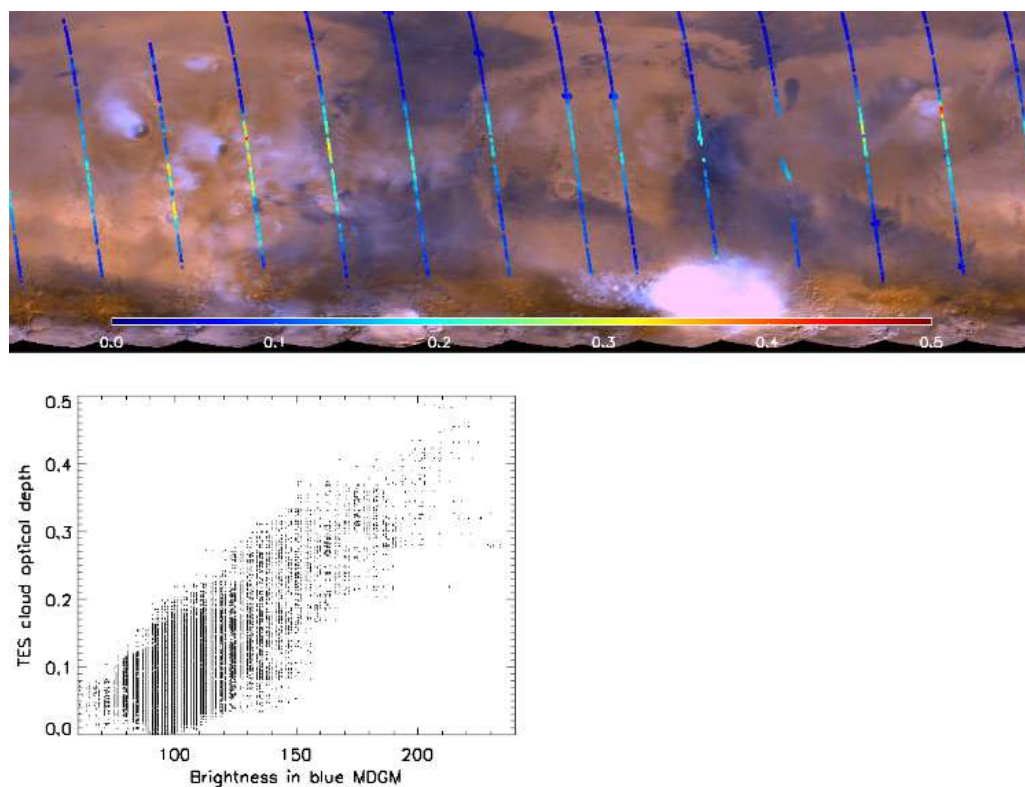
Smithsonian Astrophysical Observatory, Harvard-Smithsonian Center for Astrophysics, Cambridge, MA 02138, USA; ggonzalezabad@cfa.harvard.edu

\* Correspondence: hwang@cfa.harvard.edu

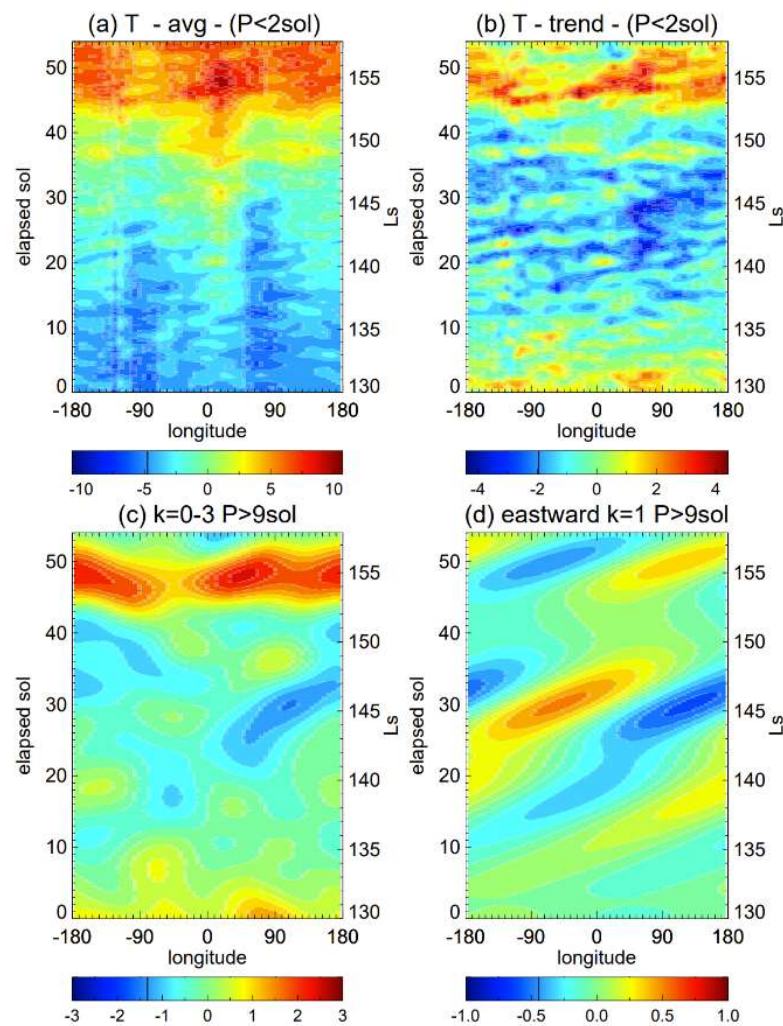
**Supplementary Materials:** The following are available online at [www.mdpi.com/article/10.3390/geosciences11080324/s1](http://www.mdpi.com/article/10.3390/geosciences11080324/s1), Figure S1: Histograms of the B channel adjusted Data Numbers, Figure S2: Relationship between the DNs of the B channel MGS MDGM and the MGS TES cloud optical depths, Figure S3: Eddy temperatures derived from the EMARS data assimilation product Figure S4: Longitude versus time evolution of cloud DN deviation in the summer of MY 29, Figure S5: Vertical variation of the difference between the 1500 LT temperature and the daily mean temperature.



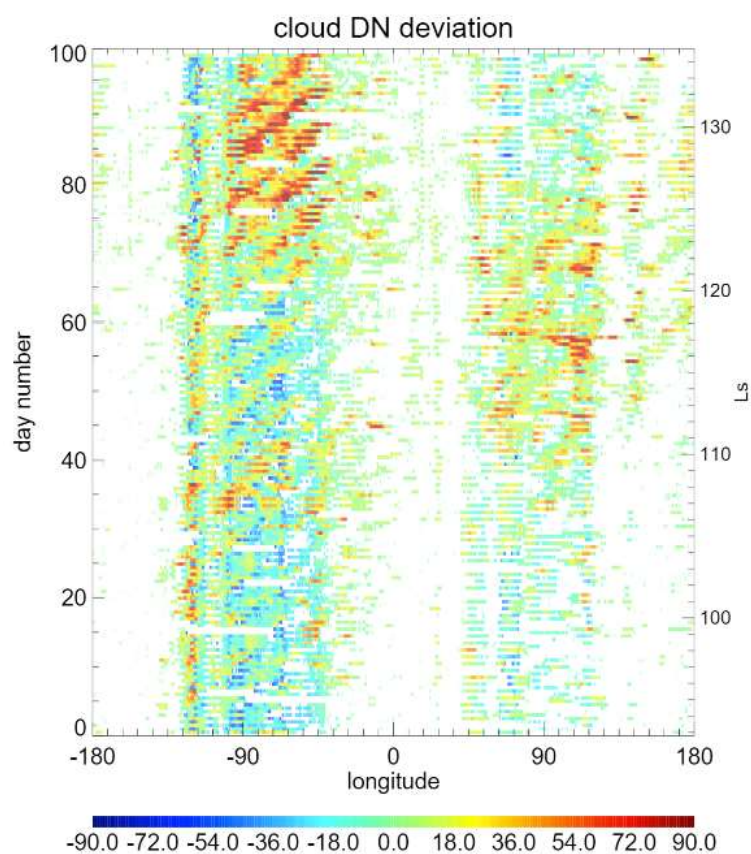
**Supplementary Figure S1.** Histograms of the B channel adjusted Data Numbers (DNs, see Section 4.3) for cloudy (red line) and non-cloudy (blue line) pixels derived from MDGMs for subphases from P01 to B01. The vertical axis is on log scale. The total number of pixels used for the plot is on the order of  $3 \times 10^9$ . The dotted black line is a Gaussian fit to the non-cloudy blue line, with a standard deviation  $\sigma$  of 7. The dashed lines indicate the corresponding modes of distributions. The distance between the modes is 29, which is about  $4\sigma$ .



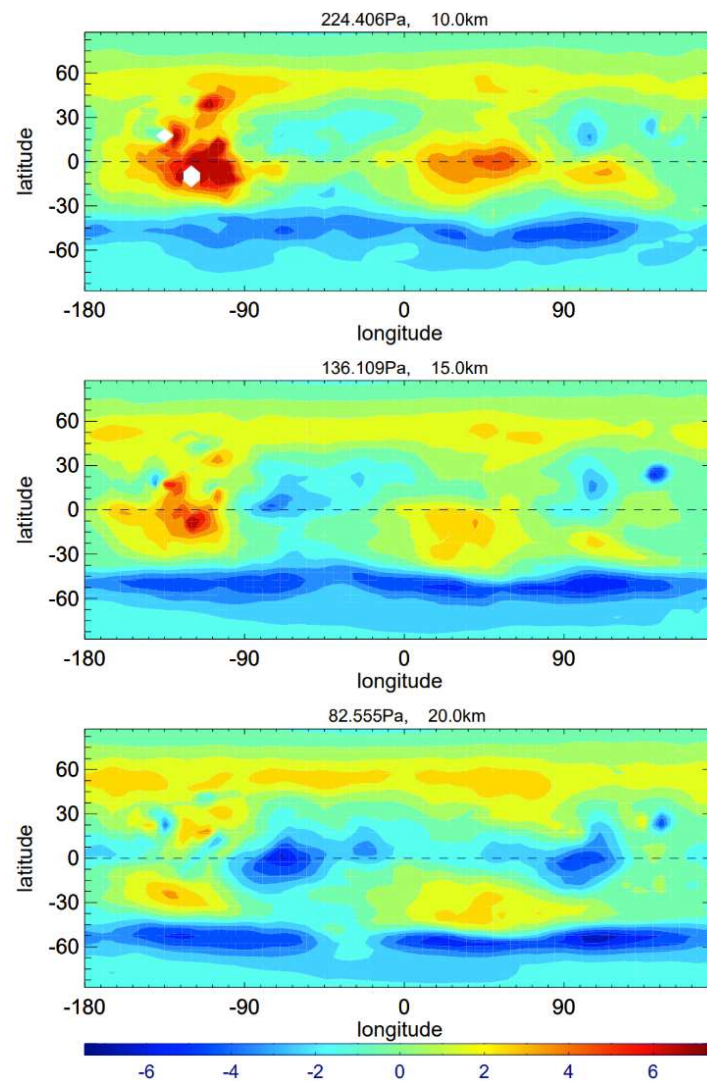
**Supplementary Figure S2.** (Top) The MGS TES cloud optical depth  $\tau$  (color bar) superimposed on the contemporaneous MGS MOC color MDGM ( $60^{\circ}$  S– $60^{\circ}$  N) for MY 25  $L_s = 95^{\circ}$ . (Bottom) Scatter plot of the TES optical depth versus the B channel MDGM brightness (as represented by Data Numbers) for the coincident data points in the top panel. Positive correlation is suggested by the data.



**Supplementary Figure S3.** Longitude versus time plots of eddy temperatures (K) derived from the EMARS data assimilation product ( $6^\circ$  longitude  $\times$   $5^\circ$  latitude) for  $2.5^\circ$  S and the  $p = 130$  Pa pressure level, with the right axis denoting  $L_s$  and the left axis denoting the sol number since the beginning of the time period. (a) Result after removing the domain average and wave period  $P < 2$  sol eddies; (b) result after removing the time trend at each longitude and the  $P < 2$  sol eddies; (c) result for zonal wavenumber  $k = 0-3$  and  $P > 9$  sol eddies during the time period; (d) result for eastward propagating  $P > 9$  sol  $k = 1$  wave during the time period.



**Supplementary Figure S4.** Highly regular  $P \approx 5$ -day waves in the cloud masks during  $L_s = 93^\circ$ – $134^\circ$  of MY 29. Results are derived in the same way as for Figure 7b of the main text. There is a possible episode of cloud brightening in the eastern hemisphere during  $L_s = 110^\circ$ – $120^\circ$  of MY 29, which is earlier than the episode listed in Table 1.



**Supplementary Figure S5.** Difference of 1500 LT temperature and daily mean temperature (color bar in Kelvin) at **(top)**  $p = 224$  Pa **(middle)**  $p = 136$  Pa, and **(bottom)**  $p = 83$  Pa. Results are derived from the OpenMARS data assimilation product for  $L_s = 105^\circ\text{--}120^\circ$  of MY 29. Blank areas in the top panel correspond to grid points that are below the surface. The equator is indicated by a black line.